# Journal of Materials Chemistry B

Accepted Manuscript



This is an *Accepted Manuscript*, which has been through the Royal Society of Chemistry peer review process and has been accepted for publication.

Accepted Manuscripts are published online shortly after acceptance, before technical editing, formatting and proof reading. Using this free service, authors can make their results available to the community, in citable form, before we publish the edited article. We will replace this Accepted Manuscript with the edited and formatted Advance Article as soon as it is available.

You can find more information about *Accepted Manuscripts* in the **Information for Authors**.

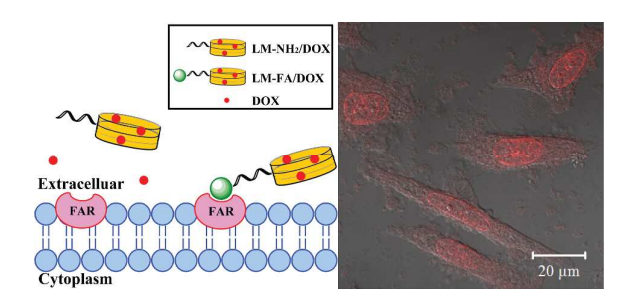
Please note that technical editing may introduce minor changes to the text and/or graphics, which may alter content. The journal's standard <u>Terms & Conditions</u> and the <u>Ethical guidelines</u> still apply. In no event shall the Royal Society of Chemistry be held responsible for any errors or omissions in this *Accepted Manuscript* or any consequences arising from the use of any information it contains.



Table of Contents (TOC) Image

## Folic acid-modified laponite nanodisks for targeted anticancer drug delivery $\mbox{\dagger}$

Yilun Wu,<sup>a</sup> Rui Guo,<sup>a</sup> Shihui Wen,<sup>a</sup> Mingwu Shen,<sup>a</sup> Meifang Zhu,<sup>b</sup> Jianhua Wang,<sup>c</sup> Xiangyang Shi<sup>ab</sup>



Folic acid-modified laponite nanodisks can be used as an efficient platform for targeted delivery of doxorubicin *via* a receptor-mediated pathway.

Cite this: DOI: 10.1039/c0xx00000x

**PAPER** 

www.rsc.org/xxxxxx

### 

Yilun Wu, a Rui Guo, Shihui Wen, Mingwu Shen, Meifang Zhu, Jianhua Wang, Xiangyang Shi Ab

Received (in XXX, XXX) Xth XXXXXXXXX 20XX, Accepted Xth XXXXXXXX 20XX 5 DOI: 10.1039/b000000x

We report here an effective approach to modifying laponite (LAP) nanodisks with folic acid (FA) for targeted anticancer drug delivery applications. In this approach, LAP nanodisks were first modified with 3-aminopropyldimethylethoxysilane (APMES) to render them with abundant surface amines, followed by conjugation with FA *via* 1-ethyl-3-(3-dimethylaminopropyl) carbodiimide (EDC) chemistry. The formed FA-modified LAP nanodisks (LM-FA) were then used to encapsulate anticancer drug doxorubicin (DOX). The surface modification of LAP nanodisks and the subsequent drug encapsulation within the LAP nanodisks were characterized *via* different techniques. We show that the LM-FA is able to encapsulate DOX with an efficiency of 92.1 ± 2.2%, and the formed LM-FA/DOX complexes are able to release DOX in a pH-dependent manner with a higher DOX release rate under an acidic pH condition than under a physiological pH condition. The encapsulation of DOX within LM-FA does not compromise its therapeutic activity. Importantly, the formed LM-FA/DOX complexes are able to specifically target cancer cells overexpressing high-affinity FA receptors as confirmed *via* flow cytometric analysis and confocal microscopic observation, and exert specific therapeutic efficacy to the target cancer cells. The developed FA-modified LAP nanodisks may hold great promise to be used as an efficient nanoplatform for targeted delivery of different anticancer drugs.

#### Introduction

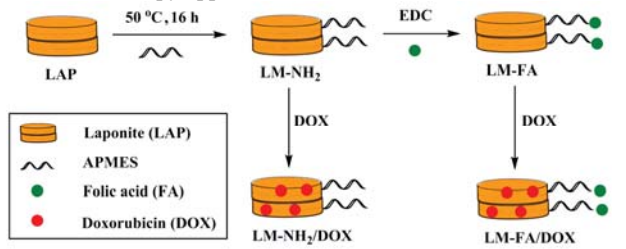
Most of the currently used anticancer drugs lack sufficient water solubility, have limited bioavailability, and display nonspecificity, quite limiting their clinical applications. For effective 25 cancer therapy applications, it is essential to develop a carrier system that is able to improve the water solubility of the drug and enables targeted delivery of the drug to cancer cells via a receptor-mediated pathway. Recent advances in micro and nanotechnology show that polymer microparticles nanoparticles (NPs),<sup>2-6</sup> micelles,<sup>7, 8</sup> nanogels,<sup>9, 10</sup> liposomes,<sup>11</sup> dendrimers,<sup>12-17</sup> and composite nanofibers<sup>18, 19</sup> can be used for anticancer drug delivery applications. Similarly, some inorganic nanoparticulate systems such as iron oxide NPs,20 carbon nanotubes, 21, 22 mesoporous silica NPs, 23, 24 zirconium phosphate 35 nano-platelets, 25 and laponite (LAP) nanodisks 26 have also been investigated as new platforms for anticancer drug delivery applications. Compared with the organic nanoparticulate systems, the used inorganic carrier system may offer great advantages such as the robust stability in the physiological conditions in terms of 40 the shape, conformation, and physicochemical properties, higher encapsulation capacity due to their unique surface<sup>21</sup> or internal structures.<sup>26</sup> Therefore, development of different inorganic nanocarrier systems for anticancer drug delivery is of paramount importance.

Laponite (LAP) is a synthetic biodegradable layered

aluminosilicate disk-like clay material. <sup>27-30</sup> The interlayer space of LAP can be used for effective drug encapsulation, which affords LAP nanodisks as an ideal carrier system for different applications. <sup>31-35</sup> For instance, a hydrophobic drug itraconazole was able to be incorporated into LAP to have a sustained release profile. <sup>31, 32</sup> LAP nanodisks encapsulated with an antibiotic, amoxicillin can be further incorporated within electrospun poly(lactic-co-glycolic acid) nanofibers to have improved release kinetics for antibacterial applications. <sup>34</sup>

In our previous work, we have shown that DOX can be encapsulated within LAP nanodisks with a high drug encapsulation efficiency.<sup>26</sup> The formed LAP/DOX complexes displayed enhanced antitumor activity in vitro, presumably due to the enhanced intracellular uptake of the LAP/DOX complexes. 60 Given the fact that the LAP's silanol groups can be functionalized via silanization to render the LAP nanodisks with abundant amine groups, 36 it's possible to modify the LAP nanodisks with targeting ligands for targeted drug delivery applications. Our previous work has shown that aminated dendrimers or inorganic 65 NPs can be readily modified with folic acid (FA) via 1-ethyl-3-(3-dimethylaminopropyl) carbodiimide hydrochloride (EDC) chemistry for targeted drug/gene delivery16, 17, 37-39 or molecular imaging<sup>40-42</sup> applications. These prior work and successes in the preparation of FA-modified NPs lead us to hypothesize that 70 amine-functionalized LAP nanodisks via silanization may be able to be further functionalized with FA, thereby providing a targeted drug delivery system for therapeutic inhibition of cancer cells overexpressing folic acid receptors (FAR).

In this present study, LAP nanodisks were first silanized *via* 3saminopropyldimethylethoxysilane (APMES) to render them with
abundant surface amine groups. The aminated LAP nanodisks
were then modified with FA *via* EDC chemistry (Scheme 1). The
formed FA-modified LAP nanodisks (LM-FA) were then used to
encapsulate DOX. The formed LM-FA and LM-FA/DOX
complexes were characterized *via* different techniques. The
release of DOX from LM-FA/DOX complexes was investigated
under different pH conditions. Finally the antitumor efficacy and
the performance of FA-mediated targeted delivery of LMFA/DOX complexes were investigated *via* cell viability assay,
flow cytometric analysis, and confocal laser scanning
microscopic (CLSM) observation. To our knowledge, this is the
first attempt to develop LAP-based targeted drug delivery system
for cancer therapy applications.



20 Scheme 1. Schematic illustration of the design and preparation of LM-NH<sub>2</sub>/DOX and LM-FA/DOX complexes.

#### **Experimental**

#### Materials

LAP with known empirical formula  $^{25}\ Na^{+0.7}[(Si_8Mg_{5.5}Li_{0.3})O_{20}(OH)_4]^{-0.7} \ \ and \ \ DOX \ \ were \ \ purchased$ from Zhejiang Institute of Geologic and Mineral Resources (Hangzhou, China) and Beijing Huafeng Pharmaceutical Co., Ltd. (Beijing, China), respectively. APMES and EDC were from J&K Chemical Ltd. (Shanghai, China). Resazurin and Hoechst 33342 30 were from Sigma-Aldrich (St. Louis, MO). All other chemicals and reagents were from Sinopharm Chemical Reagent Co., Ltd (Shanghai, China). The cell culture flasks and plates were from NEST Biotechnology (Shanghai, China). All chemicals and materials were used as received. HeLa cells (a human cervical 35 cancer cell line) and L929 cells (a mouse fibroblast cell line) were obtained from Institute of Biochemistry and Cell Biology (the Chinese Academy of Sciences, Shanghai, China). Dulbecco's modified eagle medium (DMEM), fetal bovine serum (FBS), penicillin, and streptomycin were from Hangzhou Jinuo 40 Biomedical Technology (Hangzhou, China). Water used in all experiments was purified using a Milli-O Plus 185 water purification system (Millipore, Bedford, MA) with resistivity higher than 18 M $\Omega$ ·cm. Regenerated cellulose dialysis membranes (MWCO = 14 000) were acquired from Fisher 45 (Waltham, MA).

#### Synthesis of FA-modified LAP nanodisks

LAP was dispersed in water and sonicated (50 W, SK1200H, Shanghai KUDOS Inc., China) at room temperature to get an aqueous solution at a concentration of 10 mg/mL. An aqueous

solution of APMES (1 mL, 124 μM) was added into the LAP suspension (5 mL, 10 mg/mL) under magnetic stirring. This reaction was maintained at 50 °C using a water bath for 16 h according to a procedure described in the literature.<sup>36</sup> Then the reaction mixture was extensively dialyzed against phosphate buffered saline (PBS) (6 times, 2 L) and water (6 times, 2 L) for 4 days using a dialysis membrane with MWCO of 14 000, yielding a semi-transparent suspension of APMES-modified LAP nanodisks (LM-NH<sub>2</sub>). The concentration of the LM-NH<sub>2</sub> was calculated by lyophilization of a portion of the LM-NH<sub>2</sub> os suspension with a given volume.

Then FA was modified onto the surface of LM-NH<sub>2</sub> *via* EDC chemistry according to protocols described in our previous work. <sup>14</sup> In brief, FA (3.5 mg, 8 µmol) dissolved in 2 mL DMSO was mixed with a DMSO solution of EDC (3 mL, 20 mg, 100 mg) under magnetic stirring for 3 h. Subsequently, the activated FA was added to an aqueous suspension of LM-NH<sub>2</sub> (6.5 mg/mL, 5.4 mL) under vigorous magnetic stirring. The reaction was continued for 3 days. Then, the reaction mixture was purified according to the procedure describe above to get a semi-70 transparent suspension of LM-FA product.

#### **Encapsulation of DOX within LM-FA nanodisks**

The procedure to encapsulating DOX within LM-FA nanodisks was similar to that described in our previous report.<sup>26</sup> Briefly, an aqueous DOX solution (2 mg/mL, 1 mL) was added into an 75 aqueous suspension of LM-FA (6 mg/mL, 1 mL) under magnetic stirring for 24 h. An optimized mass ratio of LM-FA/DOX at 3:1 was employed according to our previous work.26 The LM-FA/DOX complexes were obtained by centrifugation (8000 rpm, 5 min) and rinsing with water for 3 times, and stored in dark at 4 80 °C before use. The DOX encapsulation efficiency can be calculated by measuring the concentration of free DOX in the collected supernatants after 4 times of centrifugation by Lambda 25 UV-vis spectrophotometer (PerkinElmer, Waltham, MA) at 480 nm using a standard DOX absorbance-concentration 85 calibration curve. For comparison, non-targeted LM-NH<sub>2</sub>/DOX complexes were also prepared under similar experimental conditions. The DOX encapsulation efficiency and percentage can be calculated by Eq. (1) and Eq. (2), respectively.

Encapsulation efficiency =  $(M_t/M_0) \times 100\%$  (1)

Encapsulation percentage =  $(M_t/M_L) \times 100\%$  (2) where  $M_t$ ,  $M_0$ , and  $M_L$  stand for the masses of the encapsulated DOX, the initial DOX, and the LAP carrier, respectively.

#### Characterization

Thermogravimetric analysis (TGA) was performed to characterize the surface modification of APMES and FA onto the LAP nanodisks using a TG 209 F1 (NETZSCH Instruments Co., Ltd., Germany) thermogravimetric analyzer. The samples were heated from room temperature to 900 °C at a rate of 20 °C /min under air. The initial masses of LAP, LM-NH<sub>2</sub>, and LM-FA were 6.82 mg, 4.56 mg, and 5.03 mg, respectively. To determine the density of the amine groups on the surfaces of LM-NH<sub>2</sub> and LM-FA, the LM-NH<sub>2</sub> and LM-FA were dispersed in water. Then Megazyme's Primary Amino Nitrogen (PANOPA) Assay Kit (Bray, Ireland, <a href="https://www.megazyme.com">www.megazyme.com</a>) was used to determine the density of their primary amines according to the manufacturer's instruction. The principle of this assay has been validated in the

literature. 43-45 Zeta-potential and dynamic light scattering (DLS) measurements were carried out using a Zetasizer Nano ZS system (Malvern, Worcestershire, UK) equipped with a standard 633 nm laser. All experiments were done in triplicate. The crystalline structures of LAP, LM-NH2, and LM-FA nanodisks were characterized by a Rigaku D/max-2550 PC X-ray diffraction (XRD) system (Rigaku Co., Tokyo, Japan) using Cu Kα radiation with a wavelength of 1.54 Å at 40 kV and 200 mA. The scan was performed from 5° to 60° (2θ). The plane spacing of different 10 diffraction plane (dhkl) can be calculated from Bragg's law. Transmission electron microscopy (TEM) was performed using a JEOL 2010F analytical electron microscope (JEOL, Tokyo, Japan) operating at 200 kV. TEM samples were prepared by dropping a dilute particle suspension (6 µL) onto a carbon-coated copper grid 15 and air-dried before measurements. UV-vis spectra were collected using a PerkinElmer Lambda 25 UV-vis spectrophotometer. Samples of LAP, LM-NH<sub>2</sub>, LM-FA, LM-NH<sub>2</sub>/DOX, and LM-FA/DOX were dispersed in water before measurement.

#### 20 In vitro drug release

The in vitro release kinetics of DOX from LM-NH<sub>2</sub>/DOX and LM-FA/DOX complexes under two different pH conditions were monitored using UV-vis spectrometry. Briefly, LM-NH<sub>2</sub>/DOX or LM-FA/DOX complexes (2 mg) dispersed into 1 mL PBS 25 solution (0.2 M, pH = 7.4) or 1 mL citric acid-disodium hydrogen phosphate buffer (0.2 M, pH = 5.0) were placed in a dialysis bag with MWCO of 14 000, and suspended in the corresponding buffer medium (9 mL) in a sample vial. All samples were incubated in a vapor-bathing constant temperature vibrator at 37 <sup>30</sup> °C. At the predetermined time interval, 1 mL buffer solution was taken out from the outer phase of each sample vial and equal volume of the corresponding buffer solution was replenished in the sample vial. The released DOX was quantified using UV-vis spectroscopy at 480 nm using the corresponding buffer solution 35 as background. The release experiment was done in triplicate.

#### Cell culture and cytotoxicity assay

HeLa cells were continuously cultured in 25 cm<sup>2</sup> tissue culture flasks with 5 mL DMEM containing 10% FBS, 100 U/mL penicillin, and 100 µg/mL streptomycin in a humidified incubator 40 with 5% CO<sub>2</sub> at 37 °C. Note that in all cell biology experiments, folic acid-free medium was used. To test the cytotoxicity of LM-NH<sub>2</sub> and LM-FA nanodisks, resazurin reduction assay of HeLa cells was performed after treatment with the nanodisks at different concentrations. Briefly, HeLa cells were seeded in 96-<sup>45</sup> well plates in 200 μL fresh medium with a density of  $1 \times 10^4$  cells per well the day before the experiment. The next day, the medium was replaced with 200 µL fresh medium containing 20 µL PBS solutions of LM-NH2 or LM-FA nanodisks with different final concentrations. PBS was used as control. After 24 h, the medium 50 was discarded and the cells were washed with PBS for 3 times, followed by addition of 200 µL fresh DMEM containing 20 µL resazurin (with a final concentration of 0.1 mg/mL). After incubation of the cells at 37 °C for additional 4 h, 100 µL of supernatant from each well was transferred to each well in a black 55 96-well plate. A multifunctional ELIASA reader (Biotek, Synergy 2) was used to read the resorufin fluorescence ( $\lambda_{ex} = 530$ 

nm,  $\lambda_{em}$  = 590 nm). Mean and standard deviation for the triplicate wells of each sample were recorded.

To check the therapeutic efficacy of LM-NH<sub>2</sub>/DOX and LM-60 FA/DOX complexes, the viability of HeLa cells treated with the complexes at different DOX concentrations were analyzed by resazurin reduction assay. Free DOX under the same concentrations was also tested for comparison. HeLa cells were seeded in 96-well plates in 200 µL fresh medium with a density <sub>65</sub> of  $1 \times 10^4$  cells per well. After overnight culture to bring the cells to confluence, the medium was replaced by the mixture of 180 µL DMEM and 20  $\mu$ L PBS solutions of free DOX, LM-NH<sub>2</sub>/DOX or LM-FA/DOX complexes at the final DOX concentration of 0.5, 2.0, 6.0, 10.0, 20.0, and 25.0 µg/mL, respectively. The cells were 70 then incubated for 24 h, followed by resazurin reduction assay according to the protocols described above. Mean and standard deviation for the triplicate wells of each sample were recorded.

#### FA-mediated specific delivery of DOX to cancer cells

To check the performance of FA-mediated targeting delivery of 75 DOX using LM-FA/DOX complexes, HeLa cells were seeded in 200  $\mu$ L DMEM in 96-well plate with a density of  $1 \times 10^4$  per well. After cultured for 24 h to bring the cells to confluence, the medium was replaced with 200 µL fresh medium containing free DOX, LM-NH<sub>2</sub>/DOX, and LM-FA/DOX at a final DOX 80 concentration of 10 μg/mL. After 4 h, the cells were washed with PBS for 3 times and 200  $\mu L$  fresh DOX-free DMEM was added and the cells were continuously cultured for another 24 h and 48 h, respectively. The viability of cells was measured using resazurin reduction assay according to protocols described above.

The targeting specificity of LM-FA/DOX complexes was quantitatively analyzed via flow cytometry. HeLa cells were seeded in a 12-well tissue culture plate with a density of  $2 \times 10^5$ cells per well. After 24 h incubation, the medium was replaced with fresh medium containing free DOX, LM-NH<sub>2</sub>/DOX, or LM-90 FA/DOX complexes at a final DOX concentration of 6 µg/mL. After 4 h incubation, the medium was discarded and the cells were rinsed with PBS for 3 times, trypsinated, centrifuged, and resuspended in 1 mL PBS. L929 cells that do not express FAR<sup>46</sup> 47 were also used for comparison. The intensity of DOX 95 fluorescence was subsequently measured by FACS Calibur flow cytometer (Becton Dickinson, Mountain View, CA) equipped with a 15 mW, 488 nm, and air-cooled argon ion laser. The fluorescent emission was collected through a 575 nm band-pass filter and acquired in log mode. For each sample,  $1 \times 10^4$  cells 100 were measured, and the measurement was performed in triplicate. Cells treated with PBS were also measured as a blank control.

The intracellular uptake of DOX was observed by CLSM (Carl Zeiss LSM 700, Jena, Germany). Cover slips with a diameter of 14 mm were pretreated by 5% HCl, 30% HNO<sub>3</sub>, and 75% alcohol, 105 placed in 24-well tissue culture plates, and then soaked by DMEM overnight. HeLa or L929 cells were seeded into each well with a density of  $2 \times 10^5$  cells per well. After 48 h culture to allow the cells well attached onto the coverslips, the cells were treated with free DOX, LM-NH2/DOX, or LM-FA/DOX 110 complexes at a final DOX concentration of 6 µg/mL for 4 h. Then the HeLa or L929 cells were fixed with glutaraldehyde (2.5%) for 15 min at 4 °C and counterstained with Hoechst 33342 (1 µg/mL) for 15 min at 37 °C using a standard procedure. Finally, samples

were imaged using a 63× oil-immersion objective lens.

To further confirm the targeted cellular uptake of LM-FA nanodisks, HeLa and L929 cells were seeded in 2 mL DMEM in 6-well plate at a density of 2 ×10<sup>5</sup> cells per well. After cultured 5 for 12 h to bring the cells to confluence, the medium was replaced with 2 mL fresh DMEM containing LM-NH<sub>2</sub> (0.1 mL, 1 mg/mL) or LM-FA (0.1 mL, 1 mg/mL). After 4 h, the cells were rinsed with PBS for 3 times, harvested, counted, and lysed using an aqua regia solution (0.5 mL) for 6 h. Finally the cellular Si uptake, which is associated with the LAP uptake was quantified by Leeman Prodigy inductively coupled plasma-optical emission spectroscopy (ICP-OES, Hudson, NH). Cells treated with 2 mL fresh DMEM containing 0.1 mL PBS were used as control. All the experiments were done in triplicate.

#### 15 Statistical analysis

One-way ANOVA statistical analysis was performed to evaluate the significance of the experimental data. 0.05 was selected as the significance level, and the data were indicated with (\*) for p < 0.05, (\*\*) for p < 0.01, and (\*\*\*) for p < 0.001, respectively.

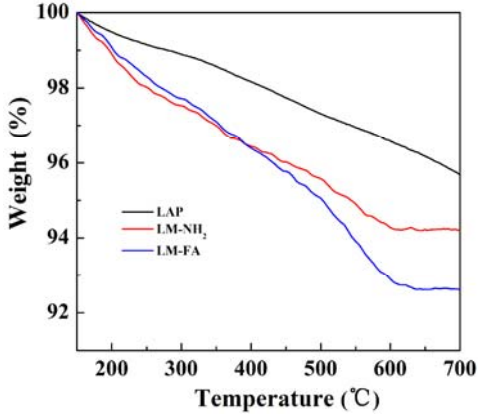
#### 20 Results and discussion

#### Formation of FA-modified LAP nanodisks

To render LAP nanodisks with targeting specificity, the LAP nanodisks were first silanized to render them with abundant surface amines, followed by modification with FA via EDC 25 chemistry (Scheme 1). FA was selected as a targeting ligand that can specifically target a range of FAR-overexpressing human carcinomas, such as breast, ovary, endometrium, kidney, lung, head and neck, brain, and myeloid cancers. 48, 49 The modification of APMES onto the surface of LAP to form LM-NH2 and the 30 subsequent conjugation with FA was first confirmed by TGA (Figure 1). Due to the fact that no apparent weight loss of LM-NH<sub>2</sub> and LM-FA occurred at 700 °C, we chose this temperature for quantification of APMES and FA grafting, in agreement with that reported in the literature.<sup>36</sup> By comparison with the pristine <sub>35</sub> LAP, the aminated LM-NH<sub>2</sub> has a weight loss of 1.48% at 700 °C, suggesting that 1.48% APMES has been modified onto the surface LAP. Furthermore, by subtracting the residue weight of APMES-modified LAP (LM-NH<sub>2</sub>) at 700 °C, the amount of FA modification was estimated to be 1.62% for the final LM-FA 40 product. Overall, the TGA results suggest that LM-NH2 and LM-FA have been successfully synthesized. The density of the primary amines of LM-NH2 and LM-FA measured via PANOPA assay reveals that the grafting of FA onto the LM-NH2 significantly reduces the amine density (53.79 versus 86.33 45 µmol/g). The percentage of non-reacted NH<sub>2</sub> groups was calculated to be 62.3%. These results are consistent with the TGA data. Note that the amine of FA grafted onto the LAP surface does not affect the PANOPA assay, because the FA amine has a quite low activity from the structural point of view and is unable 50 to be effectively detected by the PANOPA assay. To validate this statement, we used PANOPA assay to analyze the -NH2 of free FA (with a known amount of 2.5×10<sup>-8</sup> mol) dissolved in PBS. Our results showed that only 4.2×10<sup>-10</sup> mol of -NH<sub>2</sub> (1.68% of

Zeta potential measurements were used to monitor the surface potential changes after silanization of LAP and the subsequent

FA conjugation (Table 1). When compared with the pristine LAP with a quite negative surface potential (-37.9  $\pm$  1.31 mV), the silanization step renders the formed LM-NH<sub>2</sub> with significantly 60 increased surface potential (-2.44  $\pm$  0.89 mV). It is interesting to note that the silanization step is unable to reverse the surface potential of LAP, which may be due to the inherent large negative potential of the LAP. Further conjugation of FA does not seem to make the formed LM-FA with appreciably altered surface 65 potential (-5.37  $\pm$  1.38 mV). The hydrodynamic sizes of LAP, LM-NH<sub>2</sub>, and LM-FA were measured via DLS (Table 1). It is clear that the original LAP has a hydrodynamic size of  $40.7 \pm 0.3$ nm, while the silanization step affords the LAP with increased size  $(76.6 \pm 4.5 \text{ nm for LM-NH}_2)$ . The modification of FA onto 70 the surface of LM-NH<sub>2</sub> enabled a further expanded hydrodynamic diameter of LM-FA (120.9  $\pm$  4.7 nm). This suggests that the LAP silanization and further conjugation with FA may stimulate a certain aggregation of the particles.



75 Figure 1. The TGA curves of LAP, LM-NH<sub>2</sub>, and LM-FA nanodisks, respectively.

The colloidal stability of LM-NH<sub>2</sub> and LM-FA dispersed in water was checked by monitoring the changes of their hydrodynamic sizes after stored in 7 and 30 days at 4 °C (Table S1, Electronic Supplementary Information, ESI). It can be seen that similar to the pristine LAP nanodisks, the hydrodynamic sizes of LM-NH<sub>2</sub> and LM-FA do not have any appreciable changes when compared to the freshly prepared suspensions of the corresponding particles (Table 1). Likewise, the aqueous suspensions of the pristine LAP, LM-NH<sub>2</sub>, and LM-FA are stable after one month storage (Figure S1, ESI). These results clearly suggest that the silanization of LAP and the further FA grafting do not change the colloidal stability of LAP.

**Table 1.** Zeta potential and hydrodynamic size of LAP, LM-NH<sub>2</sub>, and 50 LM-FA nanodisks. All the suspension media are water and the concentration of each suspension is 0.5 mg/mL.

Materials	Zeta potential (mV)	Hydrodynamic size (nm)	polydispersity index (PDI)
LAP	-37.9 ± 1.31	$40.7 \pm 0.3$	0.455±0.091
LM-NH <sub>2</sub>	$-2.44 \pm 0.89$	$76.6 \pm 4.5$	$0.353\pm0.031$
LM-FA	$-5.37 \pm 1.38$	$120.9 \pm 4.7$	$0.280 \pm 0.024$

The change of crystalline phase of LAP after silanization and further FA conjugation was characterized by XRD (Table S2, Figure S2, ESI). Pristine LAP shows a broad peak at  $2\theta$  of  $5.74^{\circ}$ ,

the total -NH<sub>2</sub> of free FA) was able to be detected.

Journal of Materials Chemistry B Accepted Manuscrip

The FA conjugation onto the surface of LM-NH<sub>2</sub> was 10 characterized via UV-vis spectroscopy (Figure 2). The apprearance of the featured absorbance of FA at 280 nm for LM-FA suggests the successful conjugation of FA onto the surface of LM-NH<sub>2</sub>, in agreement with the literature. <sup>16, 38, 52</sup> In contrast, the pristine LAP and LM-NH2 nanodisks do not have apparent 15 absorption features in a wavelength range of 250-700 nm. TEM was further used to characterize the morphology of the LAP before and after surface modification (Figure 3). Disk-shaped structure of LAP before and after surface modification can be clearly seen (Figures 3a, 3b, and 3c). Apparent junctions between 20 disks can be observed after the FA conjugation modification (Figure 3c).

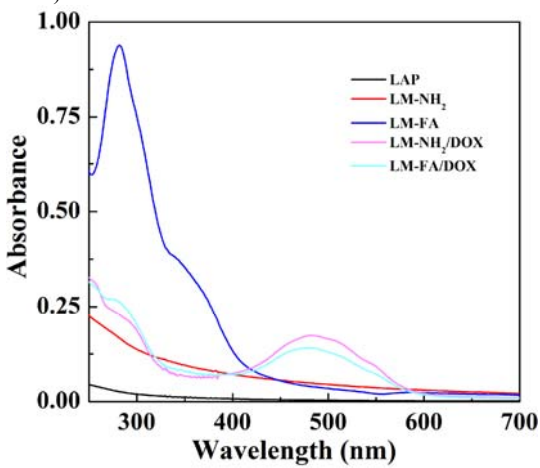


Figure 2. UV-vis spectra of LAP, LM-NH<sub>2</sub>, LM-FA, LM-NH<sub>2</sub>/DOX, and LM-FA/DOX dispersed in water.

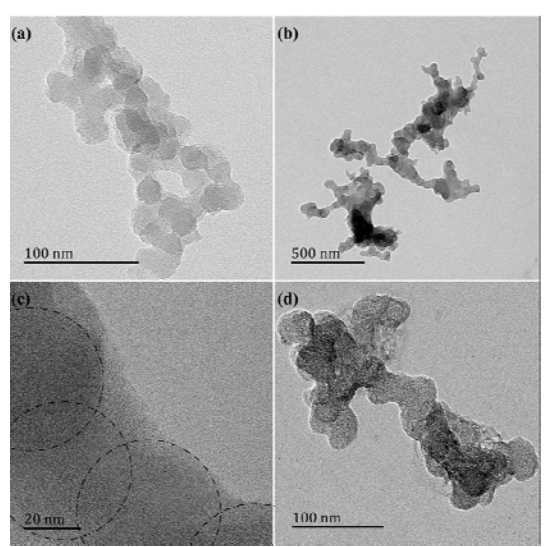


Figure 3. TEM images of (a) LAP, (b) LM-FA, and (d) LM-FA/DOX. (c) shows the high-magnification TEM image of LM-FA.

#### DOX encapsulation and release

The encapsulation of DOX within LM-NH<sub>2</sub> and LM-FA was first 30 confirmed by UV-vis spectroscopy (Figure 2). It is apparent that the encapsulation of DOX within LM-NH<sub>2</sub> and LM-FA nanodisks leads to the appearance of a featured DOX absorption peak at 480 nm, in agreement with the literature.<sup>26</sup> In contrast, without DOX encapsulation, both LM-NH2 and LM-FA nanodisks do not 35 display the DOX-associated absorption peak. Via a standard calibration curve, the DOX encapsulation efficiency was calculated to be  $87.6\pm0.65\%$  and  $92.1\pm2.2\%$  for LM-NH<sub>2</sub>/DOX and LM-FA/DOX complexes, respectively, slightly lower than that for LAP/DOX complexes reported in our previous work.<sup>26</sup> 40 This may be due to the fact that the surface modification of LAP nanodisks renders them with increased surface potential, thereby slightly decreasing the percentage of DOX adsorption onto LAP surface via electrostatic interaction. The DOX encapsulation percentages of LM-NH2/DOX and LM-FA/DOX complexes were 45 calculated to be  $22.6\pm0.17\%$  and  $23.5\pm0.56\%$ , respectively. In addition, the formation of LM-FA/DOX complexes does not seem to significantly alter the disk-shape of the LAP (Figure 3), suggesting that DOX is encapsulated within the interlayer space of the LAP nanodisks via ionic exchange. It may also be possible 50 that a portion of DOX is physically adsorbed onto the surface of LAP via electrostatic interaction and hydrogen bonding, in agreement with our previous work.<sup>26</sup>

To exert an effective therapeutic efficacy, the encapsulated DOX with LM-FA should be able to be released. We next 55 explored the release kinetics of DOX from LM-NH<sub>2</sub>/DOX and LM-FA/DOX complexes under different pH conditions (Figure 4). It can be seen that at 192 h, the cumulative release of DOX from LM-NH<sub>2</sub>/DOX complexes reaches 8.53± 0.35% and 46.19± 1.93% under pH 7.4 and pH 5.0, respectively (Figure 4a). 60 Similarly, around 7.88  $\pm$  0.55% and 39.21  $\pm$  0.81% DOX are able to be released from LM-FA/DOX complexes under pH 7.4 and pH 5.0, respectively (Figure 4b). The pH-responsive release behavior of DOX with higher DOX release rate under an acidic condition (pH = 5.0) than under the physiological condition (pH <sub>65</sub> = 7.4) should be associated with the pH-dependent hydrophilicity of DOX. Under the acidic pH condition, DOX.HCl maintains a salt form and has a very good water solubility, which affords the fast release from the interlayer space of LM-FA. In contrast, the DOX:HCl is able to be deprotonated to form a hydrophobic  $_{70}$  neutral molecule under the physiological pH condition (pH = 7.4). enabling the DOX to have a slow release rate. It is interesting to note that under similar pH conditions and time points, the cumulative release of DOX from LM-FA/DOX complexes is lower than that from LM-NH<sub>2</sub>/DOX complexes. This is likely due 75 to the fact that the FA conjugation onto the LAP surface renders additional hydrogen bonding interaction with DOX, thereby restricting the release of DOX from the LAP surfaces. Given the fact that the tumor microenvironment is slightly acidic, 18 the fast release of DOX under an acidic pH condition may be beneficial 80 for tumor therapy.

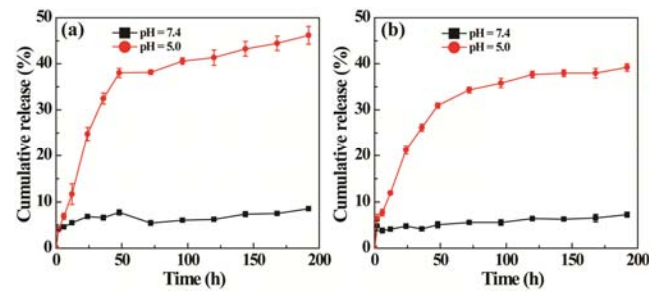


Figure 4. In vitro DOX release from (a) LM-NH2/DOX and (b) LM-FA/DOX complexes at 37 °C under different pH conditions.

#### In vitro antitumor efficacy

5 The in vitro antitumor efficacy of the LM-NH<sub>2</sub>/DOX and LM-FA/DOX complexes was evaluated by resazurin reduction assay of HeLa cells treated with the complexes (Figure 5). Both LM-NH<sub>2</sub>/DOX and LM-FA/DOX are able to significantly inhibit the growth of HeLa cells with the increase of the DOX concentration. 10 The half-maximal inhibitory concentration (IC<sub>50</sub>) of LM-NH<sub>2</sub>/DOX (10.03 μg/mL) was found to be 1.66 times higher than that of LM-FA/DOX (6.06 µg/mL). This suggests that with the FA-mediated targeting, the LM-FA/DOX complexes are able to have enhanced antitumor efficacy. It should be noted that the IC<sub>50</sub> 15 of both LM-NH<sub>2</sub>/DOX and LM-FA/DOX complexes are higher than that of free DOX (5 µg/mL) in treating HeLa cells for 24 h. This may be due to the slow release of DOX that is unable to achieve the required concentration to inhibit the cancer cell growth. The cytotoxicity of both LM-NH2 and LM-FA nanodisks 20 without DOX encapsulation was also tested via resazurin reduction assay of HeLa cells (Figure S3, ESI). It can be seen that both LM-NH<sub>2</sub> and LM-FA do not seem to be cytotoxic to HeLa cells in the studied concentration range (10-100 µg/mL). Our results suggest that the antitumor efficacy of both LM-NH<sub>2</sub>/DOX 25 and LM-FA/DOX complexes are solely associated with the encapsulated DOX drug.

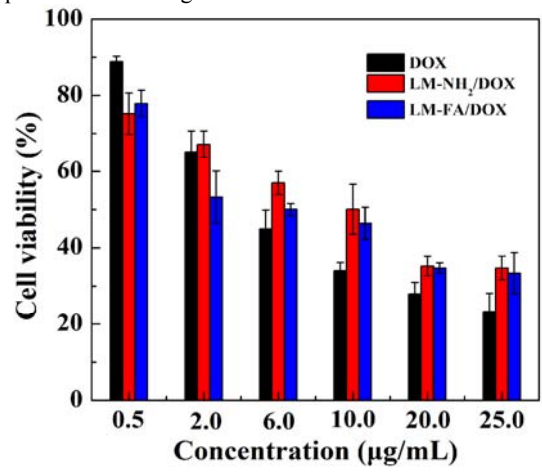


Figure 5. Resazurin reduction assay of HeLa cells treated with free DOX, LM-NH2/DOX, and LM-FA/DOX at different DOX concentrations for 24 30 h, respectively.

#### FA-targeted cellular uptake and antitumor efficacy

To further confirm the FA-mediated targeted antitumor efficacy, HeLa cells were first treated with LM-NH<sub>2</sub>/DOX and LM-FA/DOX complexes for 4 h. Then, the cell medium was replaced 35 with DOX-free fresh medium and the cells were incubated in the absence of unbounded complexes for additional 24 h and 48 h, respectively before resazurin reduction assay of the cell viability (Figure 6). PBS and free DOX were also used as control. It is clear that in all cases, longer incubation of HeLa cells treated 40 with free DOX, LM-NH2/DOX complexes, and LM-FA/DOX complexes results in more enhanced antitumor efficacy. Free DOX-treated HeLa cells have quite higher viability than those treated with LM-NH<sub>2</sub>/DOX and LM-FA/DOX complexes under similar conditions, suggesting the limited cellular uptake of free 45 DOX within 4 h. This is because the LAP/DOX complexes have a better cellular internalization capacity than free DOX.26 Under the similar conditions, the viability of HeLa cells treated with LM-FA/DOX complexes is significantly lower than that treated with LM-NH<sub>2</sub>/DOX complexes (p < 0.01). Our results further 50 indicated the role played by FA-mediated targeting that affords enhanced antitumor efficacy.

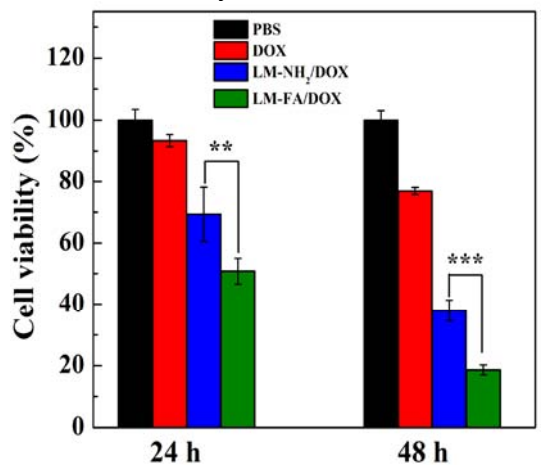


Figure 6. Resazurin reduction assay of HeLa cells treated with free DOX, LM-NH<sub>2</sub>/DOX, and LM-FA/DOX at a DOX concentration of 10 μg/mL 55 for 4 h, followed by replacing the cell medium with DOX-free fresh medium and incubating the cells for another 24 h and 48 h, respectively.

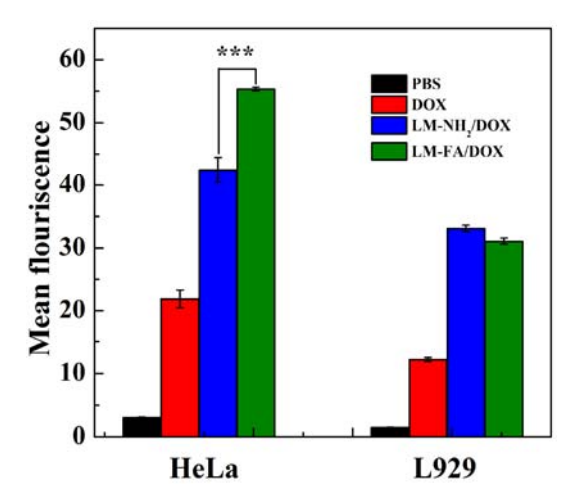


Figure 7. Flow cytometric analysis of both L929 and HeLa cells treated with free DOX, LM-NH $_2$ /DOX, and LM-FA/DOX at a DOX 60 concentration of 6 µg/mL for 4 h, respectively.

To confirm the FA-mediated specific targeting of LM-FA/DOX complexes, HeLa cells were treated with LM-FA/DOX and LM-NH<sub>2</sub>/DOX complexes for 4 h and the cells were rinsed with PBS and harvested for flow cytometric analysis based on the

fluorescence signal associated with DOX (Figure S4, ESI). 53 PBS and free DOX were used as controls. For comparison, normal L929 cells with low FAR expression were also tested under similar experimental conditions. Figure 8 shows the comparison 5 of the mean fluorescence of HeLa and L929 cells treated with free DOX, LM-NH<sub>2</sub>/DOX, and LM-FA/DOX for 4 h. Compared to the PBS control, an apparent enhancement of mean fluorescence in both HeLa and L929 cells can be observed after the treatment of free DOX and DOX complexes. The LM-10 NH<sub>2</sub>/DOX and LM-FA/DOX complexes appear to have more enhanced cellular uptake for both cells when compared with free DOX. Importantly, the mean fluorescence of HeLa cells treated with LM-FA/DOX complexes was about 1.30 times higher than that treated with LM-NH<sub>2</sub>/DOX complexes. In contrast to HeLa 15 cells having high-level FAR expression, normal L929 cells without FAR expression treated with either LM-FA/DOX or LM-NH<sub>2</sub>/DOX complexes display similar fluorescence intensity. Our results confirmed the role played by FA-mediated targeting, affording enhanced cellular uptake of LM-FA/DOX complexes.

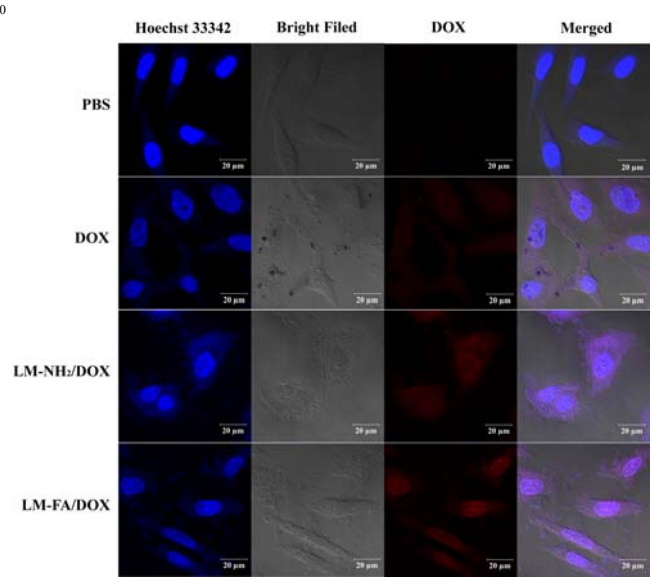


Figure 8. CLSM images of HeLa cells treated with PBS, free DOX, LM-NH2/DOX, and LM-FA/DOX with a DOX concentration of 6 µg/mL for 4 h, respectively.

The targeting specificity of LM-FA complexes was further characterized by CLSM observation of HeLa cells treated with the complexes (Figure 8). In contrast to HeLa cells treated with PBS that only display Hoechst 33342-counterstained blue fluorescence of cell nuclei, HeLa cells treated with free DOX, 30 LM-NH<sub>2</sub>/DOX, and LM-FA/DOX are able to exhibit the DOXassociated red fluorescence signal in the cytoplasma and cell nuclei. Apparently, the fluorescence intensity of the cell nuclei follows the order of LM-FA/DOX > LM-NH<sub>2</sub>/DOX > free DOX. Our CLSM results corroborate the flow cytometric analysis, 35 further demonstrating the role played by FA-mediated targeting. With the enhanced uptake of DOX in cell nuclei via FARmediated endocytosis, the LM-FA/DOX complexes are able to induce significant inhibition of the growth of cancer cells (Figure 6).<sup>54</sup> In contrast to HeLa cells with high-level FAR expression, 40 normal L929 cells without FAR expression treated with free DOX, LM-NH<sub>2</sub>/DOX, and LM-FA/DOX display approximately

similar red fluorescence signals associated with DOX uptake (Figure S5, ESI). Taken together, our results clearly suggest that the modification of FA onto LAP nanodisks enables specific 45 targeting of the LM-FA/DOX complexes to FAR-overexpressing cancer cells, thereby exerting enhanced therapeutic efficacy to the target cancer cells.

To confirm the targeted cellular uptake of LM-FA, ICP-OES was used to assess the cellualr uptake of Si element in both HeLa 50 and L929 cells (Table 2). It 's apparent that HeLa or L929 cells treated with PBS do not have any appreciable Si uptake. Under the similar experimental conditions, HeLa cells treated with LM-FA have a much higher Si uptake than those treated with LM-NH<sub>2</sub> (24.97 versus 13.98 pg/cell). In contrast, for L929 cells that 55 have a low FAR expression, the treatment of either LM-FA or LM-NH<sub>2</sub> results in approximately similar Si uptake, which is much less than that of LM-FA-treated HeLa cells. These studies further confirmed the role played by FA-mediated targeting, affording the LM-FA/DOX complexes with an ability to 60 specifically inhibit the growth of cancer cells.

Table 2. The uptake of Si element by HeLa and L929 cells treated with LM-NH<sub>2</sub> and LM-FA with a concentration of 100 µg/mL

Materials	HeLa cells (pg/cell)	L929 cells (pg/cell)
PBS	$1.28 \pm 0.43$	$1.16 \pm 0.40$
LM-NH <sub>2</sub>	$13.98 \pm 4.10$	$16.26 \pm 3.72$
LM-FA	$24.97 \pm 6.03$	$16.46 \pm 2.37$

#### **Conclusions**

In summary, we developed an LAP-based nanoplatform for 65 targeted anticancer drug delivery applications. In our approach, targeting ligand FA can be covalently conjugated onto the surface of aminated LAP nanodisks rendered by silanization via EDC chemistry. The formed LM-FA nanodisks are able to effectively encapsulate DOX with an efficiency of 92.1% and release DOX 70 in a pH-responsive manner with a higher DOX release rate at an acidic pH condition than at the physiological pH condition. The encapsulation of DOX within the FA-modified LAP nanodisks does not compromise its antitumor efficacy. Importantly, thanks to the role played by FA-mediated targeting, the formed LM-75 FA/DOX complexes are able to specifically target FARoverexpressing cancer cells and exert enhanced antitumor efficacy to the target cells. The developed FA-targeted LAP nanodisks may hold great promise to be used as a versatile platform for targeted therapy of different FAR-overexpresing 80 cancer cells in vitro and in vivo. Currently, animal experiments with solid tumor models treated with the formed LM-FA/DOX complexes are ongoing in our labortaory.

#### Acknowledgements

This research is financially supported by the National Natural 85 Science Foundation of China (81201189, 81351050, and 21273032), the Fund of the Science and Technology Commission of Shanghai Municipality (12nm0501900), the High-Tech Research and Development Program of China (2012AA030309), the Ph.D. Programs Foundation of Ministry of Education of 90 China (20130075110004), and the Program for Professor of Special Appointment (Eastern Scholar) at Shanghai Institutions of Higher Learning. Y. Wu thanks the Innovation Funds of Donghua University Master Dissertation of Excellence (EG2014019).

#### 5 Notes and references

- <sup>a</sup> College of Chemistry, Chemical Engineering and Biotechnology, Donghua University, Shanghai 201620, People's Republic of China. E-mail: xshi@dhu.edu.cn
- State Key Laboratory for Modification of Chemical Fibers and Polymer
   Materials, Donghua University, Shanghai 201620, People's Republic of China.
  - <sup>c</sup> Department of Biochemistry and Molecular & Cell Biology, School of Medicine, Shanghai Jiao Tong University, Shanghai 200025, People's Republic of China. E-mail: jianhuaw2007@gmail.com
  - $\ensuremath{\dagger}$  Electronic supplementary information (ESI) available: additional experimental results.
  - D. Peer, J. M. Karp, S. Hong, O. C. FaroKhzad, R. Margalit and R. Langer, Nat. Nanotechnol., 2007, 2, 751-760.
- K. K. Coti, M. E. Belowich, M. Liong, M. W. Ambrogio, Y. A. Lau, H. A. Khatib, J. I. Zink, N. M. Khashab and J. F. Stoddart, *Nanoscale*, 2009, 1, 16-39.
- Q.-L. Zhu, Y. Zhou, M. Guan, X.-F. Zhou, S.-d. Yang, Y. Liu, W.-L. Chen, C.-G. Zhang, Z.-Q. Yuan, C. Liu, A.-J. Zhu and X.-N. Zhang, *Biomaterials*, 2014, 35, 5965-5976.
- C. Niu, Z. Wang, G. Lu, T. M. Krupka, Y. Sun, Y. You, W. Song, H. Ran, P. Li and Y. Zheng, *Biomaterials*, 2013, 34, 2307-2317.
- W. Liu, S. Wen, L. Jiang, X. An, M. Zhang, H. Wang, Z. Zhang, G. Zhang and X. Shi, *Curr. Nanosci.*, 2014, 10, 543-552.
- W. Liu, S. Wen, M. Shen and X. Shi, New J. Chem., 2014, 38, 3917-3924.
  - 7. S. Li, W. Wu, K. M. Xiu, F. J. Xu, Z. M. Li and J. S. Li, *J. Biomed. Nanotechnol.*, 2014, **10**, 1480-1489.
  - 8. C. Y. Zhang, Y. Q. Yang, T. X. Huang, B. Zhao, X. D. Guo, J. F. Wang and L. J. Zhang, *Biomaterials*, 2012, **33**, 6273-6283.
  - 9. N. V. Nukolova, H. S. Oberoi, S. M. Cohen, A. V. Kabanov and T. K. Bronich, *Biomaterials*, 2011, 32, 5417-5426.
  - D. Maciel, P. Figueira, S. Xiao, D. Hu, X. Shi, J. Rodrigues, H. Tomas and Y. Li, *Biomacromolecules*, 2013, 14, 3140-3146.
- 40 11. S. M. Park, M. S. Kim, S. J. Park, E. S. Park, K. S. Choi, Y. S. Kim and H. R. Kim, J. Control. Release, 2013, 170, 373-379.
  - X. Shi, I. Lee, X. Chen, M. Shen, S. Xiao, M. Zhu, J. R. Baker, Jr. and S. H. Wang, Soft Matter, 2010, 6, 2539-2545.
  - Y. Wang, X. Cao, R. Guo, M. Shen, M. Zhang, M. Zhu and X. Shi, Polym. Chem., 2011, 2, 1754-1760.
  - 14. Y. Wang, R. Guo, X. Cao, M. Shen and X. Shi, *Biomaterials*, 2011, 115 **32**, 3322-3329.
  - M. Zhang, R. Guo, Y. Wang, X. Cao, M. Shen and X. Shi, *Int. J. Nanomed.*, 2011, 6, 2337-2349.
- 50 16. L. Zheng, J. Zhu, M. Shen, X. Chen, J. R. Baker, Jr., S. H. Wang, G. Zhang and X. Shi, Med. Chem. Commun., 2013, 4, 1001-1005.
  - 17. J. Zhu and X. Shi, J. Mater. Chem., 2013, **1**, 4199-4211.
  - F. Zheng, S. Wang, M. Shen, M. Zhu and X. Shi, *Polym. Chem.*, 2013. 4, 933-941.
- 55 19. K. Qiu, C. He, W. Feng, W. Wang, X. Zhou, Z. Yin, L. Chen, H. Wang and X. Mo, J. Mater. Chem. B, 2013, 1, 4601-4611.
  - M. H. El-Dakdouki, D. C. Zhu, K. El-Boubbou, M. Kamat, J. Chen, W. Li and X. Huang, *Biomacromolecules*, 2012, 13, 1144-1151.
- 21. S. Wen, H. Liu, H. Cai, M. Shen and X. Shi, *Adv. Healthcare Mater.*, 2013. **2**, 1267-1276.
- X. Zhang, L. Meng, Q. Lu, Z. Fei and P. J. Dyson, *Biomaterials*, 2009, 30, 6041-6047.
- L. Pan, Q. He, J. Liu, Y. Chen, M. Ma, L. Zhang and J. Shi, J. Am. Chem. Soc., 2012, 134, 5722-5725.
- 65 24. L. Pan, J. Liu, Q. He, L. Wang and J. Shi, *Biomaterials*, 2013, 34, 2719-2730.

- A. Díaz, V. Saxena, J. González, A. David, B. Casañas, C. Carpenter, J. D. Batteas, J. L. Colón, A. Clearfield and M. D. Hussain, *Chem. Commun.*, 2012, 48, 1754-1756.
- 70 26. S. Wang, Y. Wu, R. Guo, Y. Huang, S. Wen, M. Shen, J. Wang and X. Shi, *Langmuir*, 2013, 29, 5030-5036.
- 27. M. Jaber and J.-F. Lambert, J. Phys. Chem. Lett., 2010, 1, 85-88.
- Y. Li, D. Maciel, H. Tomás, J. Rodrigues, H. Ma and X. Shi, Soft Matter, 2011, 7, 6231-6238.
- 75 29. L. L. Hench, J. Am. Ceram. Soc., 1991, 74, 1487-1510.
  - D. W. Thompson and J. T. Butterworth, J. Colloid Interface Sci., 1992. 151, 236-243.
  - H. Jung, H. M. Kim, Y. B. Choy, S. J. Hwang and J. H. Choy, *Appl. Clay Sci.*, 2008, 40, 99-107.
- 80 32. H. Jung, H.-M. Kim, Y. B. Choy, S.-J. Hwang and J.-H. Choy, *Int. J. Pharm.*, 2008, 349, 283-290.
- C. Viseras, P. Cerezo, R. Sanchez, I. Salcedo and C. Aguzzi, *Appl. Clay Sci.*, 2010, 48, 291-295.
- 34. S. Wang, F. Zheng, Y. Huang, Y. Fang, M. Shen, M. Zhu and X. Shi, *ACS Appl. Mater. Interfaces*, 2012, **4**, 6393-6401.
- 35. K. Li, S. Wang, S. Wen, Y. Tang, J. Li, X. Shi and Q. Zhao, *ACS Appl. Mater. Interfaces*, 2014, **6**, 12328-12334.
- P. A. Wheeler, J. Wang, J. Baker and L. J. Mathias, *Chem. Mater.*, 2005, 17, 3012-3018.
- <sup>50</sup> 37. T. Xiao, W. Hou, X. Cao, S. Wen, M. Shen and X. Shi, *Biomater. Sci.*, 2013, 1, 1172-1180.
- 38. Y. Zheng, F. Fu, M. Zhang, M. Shen, M. Zhu and X. Shi, *Med. Chem. Commun.*, 2014, **5**, 879-885.
- 39. J. Zhu, L. Zheng, S. Wen, Y. Tang, M. Shen, G. Zhang and X. Shi, *Biomaterials*, 2014, **35**, 7635-7646.
- 40. J. Li, L. Zheng, H. Cai, W. Sun, M. Shen, G. Zhang and X. Shi, *Biomaterials*, 2013, **34**, 8382-8392.
- 41. C. Peng, J. Qin, B. Zhou, Q. Chen, M. Shen, M. Zhu, X. Lu and X. Shi, *Polym. Chem.*, 2013, **4**, 4412-4424.
- 100 42. H. Wang, L. Zheng, C. Peng, M. Shen, X. Shi and G. Zhang, Biomaterials, 2013, 34, 470-480.
  - 43. M. C. Prieto-Blanco, P. Lopez-Mahia and P. Campins-Falco, *Anal. Chem.*, 2009, **81**, 5827-5832.
- 44. Y. Moliner-Martinez, R. Herraez-Hernandez and P. Campins-Falco, *J. Chromatogr. A*, 2007, **1164**, 329-333.
- 45. B. C. Dukes and C. E. Butzke, *Am. J. Enol. Vitic.*, 1998, **49**, 125-134.
- J. Fan, G. Fang, X. Wang, F. Zeng, Y. Xiang and S. Wu, Nanotechnology, 2011, 22, 455102.
- 47. F. G. Gao, L. L. Li, T. L. Liu, N. J. Hao, H. Y. Liu, L. F. Tan, H. B. Li, X. L. Huang, B. Peng, C. M. Yan, L. Q. Yang, X. L. Wu, D. Chen and F. Q. Tang, *Nanoscale*, 2012, **4**, 3365-3372.
- I. G. Campbell, T. A. Jones, W. D. Foulkes and J. Trowsdale, *Cancer Res.*, 1991, 51, 5329-5338.
- 49. J. F. Ross, P. K. Chaudhuri and M. Ratnam, *Cancer*, 1994, **73**, 2432-5 2443.
- 50. J. Breu, W. Seidl and A. Stoll, Zeitschrift für anorganische und allgemeine Chemie, 2003, 629, 503-515.
- L. M. Daniel, R. L. Frost and H. Y. Zhu, J. Colloid Interface Sci., 2008, 321, 302-309.
- 120 52. J.-J. Lin, J.-S. Chen, S.-J. Huang, J.-H. Ko, Y.-M. Wang, T.-L. Chen and L.-F. Wang, *Biomaterials*, 2009, 30, 5114-5124.
  - 53. E. Yan, Y. Fu, X. Wang, Y. Ding, H. Qian, C.-H. Wang, Y. Hu and X. Jiang, *J. Mater. Chem. B*, 2011, **21**, 3147-3155.
- 54. R. L. Momparler, M. Karon, S. E. Siegel and F. Avila, *Cancer Res.*, 1976, **36**, 2891-2895.